

# Effect of TEC Variation on GPS Precise Point at Low Latitude

Rajesh Tiwari<sup>\*a</sup>, Soumi Bhattacharya<sup>a</sup>, P.K. Purohit<sup>b</sup>, and A.K. Gwal<sup>a</sup>

<sup>a</sup> Space Science Laboratory, Department of Physics Barkatullah University, Bhopal, India

<sup>b</sup> National Institute of Technical Teachers' Training & Research, Bhopal, India

**Abstract:** The ionosphere is a dispersive medium of charged particles between the satellite and the user on Earth. These dispersive ionized media play a vital role in the various applications of GPS (Global Positioning Systems) because the ionosphere directly influences transionospheric radio waves propagating from the satellite to the receiver. Solar flares affect the ionization state of the ionosphere with their high intensity. Sometimes the intensity is so severe that it accelerates the rate of ionization, resulting in ionospheric storms; during the ionospheric storms the concentration of charged particles varies. Among the various phenomena in the ionosphere, TEC (Total Electron Content) is responsible for range error which produces a time delay in the radio signal. The rate of change of TEC with respect to time is abbreviated as ROT. It is one of the parameters that express the ionospheric irregularities with respect to time. This work investigates the effect of ROT fluctuation on the precise positioning of GPS receivers during low solar activity periods in the equatorial anomaly region. Good geometry and a sufficient number of locked satellites provide more accuracy within the centimeter level, but the case may be different when there are any ionospheric storms. Even a few satellite signals passing through the ionospheric irregularities can cause a significant error in positioning. Thus, it is important to understand the ionospheric irregularities observed by GPS receivers in order to correct them. The ROT (TEC/Minute) parameter is used here to study the occurrence of TEC fluctuation and its potential effect on GPS, such as a horizontal positional error or the satellite geometry of the GPS receiver. This investigation is based on the analysis of a one-year observation of a fixed GPS receiver installed at Bhopal (23.202°N, 77.452°E), India during low solar active period in 2005. The GPS receiver used here is a GISTM-based dual frequency NovAtel OEM4 GPS receiver.

**Keywords:** ROT, Total Electron Content, GISTM.

## INTRODUCTION

The ionosphere is a region of charged particles: ions and electrons; that ranges from 50 Km to 1000 Km. The concentrations of charged particles in this region are produced by ionization of the gas present in the atmosphere, and the ionization phenomena vary with solar intensity, season, and solar cycle. Geomagnetic storms are caused by changes of solar wind parameters and, due to the coupling theory of the magnetosphere and ionosphere, the geomagnetic storms turns into ionospheric storm. Therefore, the radio wave passing through this medium becomes affected [1]. GPS technology has wide applications and a few of them require high precision, such as crustal deformation, geodesy, aviation, and emergency services. However, when the GPS signals from the satellite propagate through a disturbed ionospheric medium, their characteristics change according to the level of disturbance.

Increased knowledge of the ionospheric structure and its variability is important for precise positioning, since the ionosphere has an impact on GPS L-band radio signals, especially during perturbed geomagnetic conditions, due to its free electrons. When the ionosphere changes from its undisturbed state to more turbulent states, GPS applications are affected. Therefore, it is necessary to have real-time analysis to provide the model that will help to correct this error. At

the same time, these perturbations in the GPS signals are taken as scientific information used to investigate ionospheric scenarios. Ionospheric irregularities are typically small-to-medium-scale density fluctuations in the ionosphere that are routinely present. Various studies show that GPS signals are one of the best tools to study ionospheric activity, especially with low cost to high level of accuracy [2-5]. Various methods and applications have been discussed in which GPS technology proved to be the best tool for casting and forecasting [6-8]. There are various ways to study ionospheric irregularities; one of them is the TEC observations derived from a network of GPS stations using dual-frequency measurements. There are permanent stations under IGS which monitor ionospheric activity [7, 9]. An increase in the density of the worldwide GPS networks is well underway, especially the regional GPS networks, such as GEONET of Japan. GEONET has an average interstitial distance as short as 25 kilometers, and this has proved useful in studying ionospheric irregularities with very high time and spatial resolution as well as high precision [10-12]. The prior estimation of the electron density distribution of the Earth's ionosphere and plasmasphere is important for several reasons: the estimation and correction of propagation delays in the GPS; improving the accuracy of satellite navigation; predicting changes due to ionospheric storms; and predicting space weather effects on telecommunications.

TEC is an important descriptive quantity for the ionosphere. TEC is the total number of electrons present along a path between satellite and receiver (Eq. 1) per unit area (unit

\*Address correspondence to this author at the Space Science Lab, Department of Physics, Barkatullah University, Bhopal, India; E-mail: rajeshgps@gmail.com

of 1 TECU =  $10^{16}$  electrons/m<sup>2</sup>). GPS is used to derive TEC by observing carrier phase delays of received radio signals transmitted from satellites.

$$TEC = \int_{Receiver}^{Satellite} N \cdot ds \quad (1)$$

where 'N' is electron density.

A different scale of ionospheric irregularities can be described by using the distributive variation of the ionospheric TEC, which can be retrieved from a GPS signal. Monitoring the time-derivative of TEC (ROT, rate of change of TEC) is useful for tracing the presence of irregularities. Eq. (2) shows the algorithm to calculate ROT [13].

$$ROT = \frac{TEC_k^i - TEC_{k-1}^i}{(t_k - t_{k-1})} \quad (2)$$

where  $i$  is the visible satellite and  $k$  is the time of epoch.

Global snapshots of the irregularity distribution within 1000-2000 km of global network sites have been produced using a rate-of-TEC index (ROTI) based on the level of fluctuations in  $dLI/dt$  [13]. ROT is also useful in resolving the spatial boundary of the auroral zone at high latitudes [7].

## POSITION SOLUTION

The GPS receiver tracks the GPS satellite and the inbuilt programming of the receiver computes the pseudorange between the SV and the receiver, as in Eq. 3. The equation express how the pseudorange value is affected by clock drift, ionosphere, troposphere, multipath and noise as:

$$P = \rho + c(\delta^s - \delta_r) + d_{ion} + d_{trop} + noise + MP \quad (3)$$

where

$P$  = Pseudorange

$\rho$  = Real Range

$\delta^s$  = Satellite clock offset

$\delta_r$  = Receiver clock offset

$d_{ion}$  = Ionospheric Error

$d_{trop}$  = Tropospheric error

$MP$  = Multipath error

Ionospheric error is one of the major sources of error in GPS positioning. In the following section we will study the position solution during the ionospheric irregularities.

Fig. (1) explains the change in the range between the GPS satellite and the user, due to variation in the refractive index of the ionosphere. The figure shows that out of five locked satellites, the signals from PRN 9 and PRN 11 happened to pass through ionospheric irregularities. The signal of these satellites would cover a curved path rather than a straight line path. With a different range we get a new pseudorange ( $\rho'$ ). The position solution is computed with the intersection of the ranges from each satellite to the user as locus, so the variation in one range can diffract the point of intersection rather than the actual one with optical straight line. In our study we look upon each signal coming out of

the SV, and we find its equivalent effect on the position solution. Our study aims to establish the amount of ionospheric irregularities, the rate of change of TEC observed from several satellites together, as well as the resultant effects on horizontal errors in easting and northing. The confidence level of accuracy is computed by 3DRMS (99.9 % of accuracy) and CEP (49 % of accuracy level).

## EXPERIMENTAL SET UP AND METHODOLOGY

In December of 2003, two GISTM- (GPS Ionospheric Scintillation and TEC Monitor) based GPS receivers were installed at an equatorial station, Bhopal ( $23.202^0$  N,  $77.452^0$  E), India, as shown in Fig. (2). A NovAtel L1/L2 OEM GPS Card receiver with a NovAtel type 602 Survey Antenna was used for this study. The antenna is a Choke Ring designed to minimize the level of multipath effect. The receiver has 12 channels so it can record the data from 12 satellites at a time; it is also dual frequency, operating on L1 C/A code and L2 P code. Since the GPS receiver used here for experimentation was fixed and surveyed for about two years in various ionospheric conditions, its use eliminates each possible error in positioning. Therefore, we take this point as a fixed GPS point which is mounted on the roof of the Space Science Laboratory, Department of Physics, as shown by satellite picture in Fig. (2) obtained from Google Earth. We analyzed the horizontal error and the level of confidence in terms of DRMS & CEP (Eqs. 5 & 6) from the fixed GPS point for one year in 2005.

To explore the correlation between ionosphere and positional error, Total Electron Content (TEC) data were collected by the Space Science Laboratory, Department of Physics, during a period of low solar activity from January till December 2005. The receiver is used to monitor both ionospheric behavior and GPS performance in equatorial regions. Dual-frequency phase measurements with a 30 s interval are usually used to estimate phase fluctuations. To study the effect of the ionosphere on the GPS receiver, a rate of change TEC (ROT) of 1 min is calculated by using Eq. 2. To quantify the degree of ionospheric disturbances, the RMS of ROT were measured at 5-minute intervals by using all visible satellites.

$$RMS_{ROT} = \sqrt{\frac{\sum (ROT_i - \mu)^2}{n}} \quad (4)$$

where parameter  $n$  is the total number of observed values in 5 minutes, ROT is rate of change of TEC as defined in Eq. 2, and  $\mu$  is the average mean of ROT.

$$DRMS = \sqrt{(\sigma_{x_u})^2 + (\sigma_{y_u})^2} \quad (5)$$

$$CEP = 0.589\sigma_{x_u} + 0.589\sigma_{y_u} \quad (6)$$

To analyze the effect of the RMS of ROT on positioning, Circular Error Probability (CEP), DRMS, Horizontal Error, and Satellite Geometry are calculated with the help of Equations 5 and 6. It has been suggested that large-scale fluctuations in TEC produce disturbances which propagate through the ionosphere [14]. The use of these relatively infrequent samples enables one to study the irregularity structures on the order of kilometers. When using ROT, we thus avoid the problem of phase ambiguities.

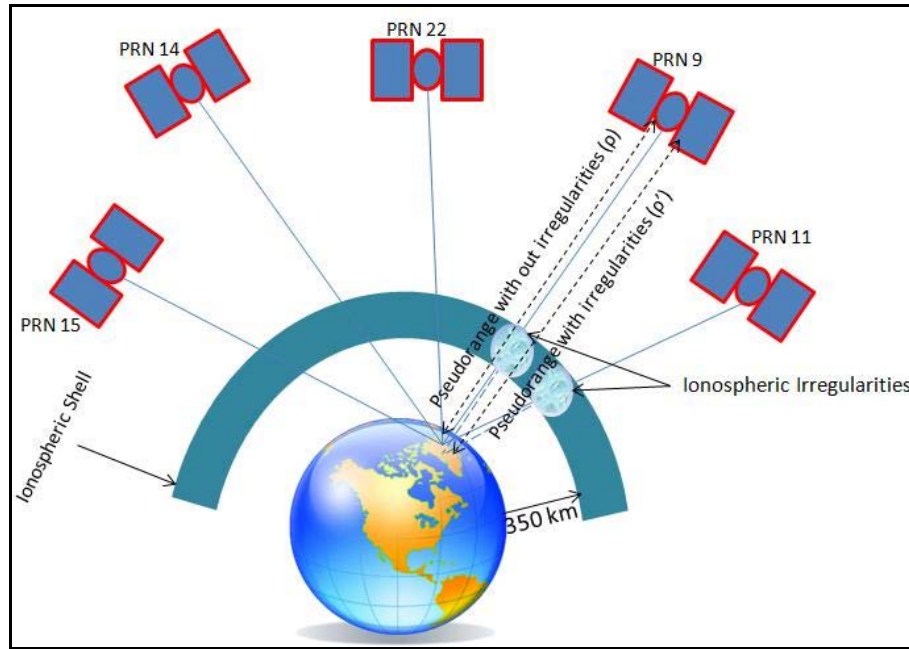


Fig. (1). Signal Path difference expressed in terms of pseudorange.

**RESULTS AND DISCUSSION**

Results have been split up into two categories based on ionospheric conditions: one is ionospheric disturbance conditions and the other is ionospheric quiet conditions. Their effect on the precise positioning of the satellite geometry of the NovAtel GPS receiver has been considered in both cases.

Fig. (3a) displays the Dst index of 24 August 2005, which was the second strongest storm of year 2005. At 06:13 UT, the sudden storm commencement (SSC) occurred for a short duration, then at 07:00 UT an initial phase was ob-

served followed by a sudden decrease in the Dst index. The main phase of the storm continued up to 12:00 UT and remained in this stage for 05 hours continuously as the Dst reached -220nT. Dst was a magnetic parameter observed near the equator, while at the same time Kp was also recorded as being high—this is the magnetic parameter recorded from the ground-based magnetometer in high latitude. During this event, the Kp index reached to a maximum magnitude of 9 during the main phase of the storm, as shown in Fig. (3b). The impact of this storm can be seen on the rate of change of TEC, as shown in the form of RMS (root mean



Fig. (2). GPS Point, Dept. of Physics Barkatullah University Bhopal.

square) of the rate of change of VTEC (ROT). As defined in Eq. 4, the RMS values of ROT for all visible satellites were calculated every 5 minutes on 24 August 2005 and are plotted in Fig. (3c). The RMS of VTEC gives an idea about the intensity and occurrence of ionospheric irregularities. The Fig. (3c) justifies that from 00:00 UT to 06:00 UT, the RMS value of ROT is less than 0.1 and is very smooth, but as soon as the SSC occurred, the RMS value of ROT started increasing and, during the main phases of the storm, it was observed to reach a maximum value of 0.58, indicating the presence of strong irregularities.

To show the effect of the above ionospheric irregularities on GPS precise positioning and on satellite geometry, Fig. (4) has been plotted in the time series for the whole day of event. The positional error recorded at Bhopal has been expressed in local frames of reference in terms of ENU (Easting Northing and Up) concerning the exact geodetic position of the fixed and well-surveyed GPS point. The left panel of Fig. (6) demonstrates the scatter plot of easting and northing errors in meter. The plot was so chosen to signify how far the position solution computed by the receiver is from the point of reference or origin (cross-section of easting and northing axis at zero). A scatter plot of 24 hours was divided into equal intervals of 06 hours and can be distinguished with different colors. Range of error was expressed in terms of the CEP, which indicates 49% of the confidence level of accuracies, while 3-DRMS is 99.9% accurate in the horizontal plane. The upper right panel shows variations of the absolute horizontal error in meters, and the number of satellites locked is shown in blue. To see the effect of ROT variation on satellite geometry, GDOP, PDOP, and HDOP have also been plotted in time series, as mentioned in the lower right panel.

Before the commencement of the initial phase of storms, the northing and easting errors are within the confidence level of 3DRMS, i.e., within 99.97% of the accuracy level.

As soon as the main phase of the commencement of the storm occurred, the Dst reached maximum negative value around 07:00 UT to 12:00 UT time, while the northing and easting errors crossed to 99.97% of the confidential of limit. The figure shows maximum position error during that time, and during the recovery phase the horizontal position converged within 99.97% of confidence levels. During this event, the 3DRMS was recorded to be 2.1686 m and CEP as 0.8892 m, which is very high for a standard GPS receiver. The absolute horizontal position error corresponding to the same time is shown on the upper right panel of the figure; it shows a similar variation, and it is clear from the figure that during the main phase of the storm, when Kp index was at its maximum, the absolute horizontal position error was observed to be more than 3 meters. This is too big to provide reliability to the user. In general, the maximum number of satellites locked by GPS is 12, but during the mentioned event the number of satellites drops down to 7, which is not bad, but due to the sudden drop of those satellites in zenith, it might disturb the satellite geometry. Fig. (4) also shows the DOP (dilution of precision) in the time series which has been categorized into GDOP (Geometry Dilution of Precision), HDOP (Horizontal Dilution of Precision), and PDOP (Position Dilution of Precision) in the right corner of the figure. The figure also gives one-to-one relation for satellite geometry and the number of locked satellite. GDOP shows the effect of the geometry of the satellites on position error, and it is roughly interpreted to be ratios of the accuracy of the position error with the user equivalent range error. It is used to provide an indication of the quality of the solution. During this event, the enhancement in position error is observed with rise of GDOP. Although the DOP's parameter appears to be fluctuating at some point, it is still within the significant range. Thus, the user may assume a position solution given by the receiver as being a correct estimation, which in fact may not be the case.

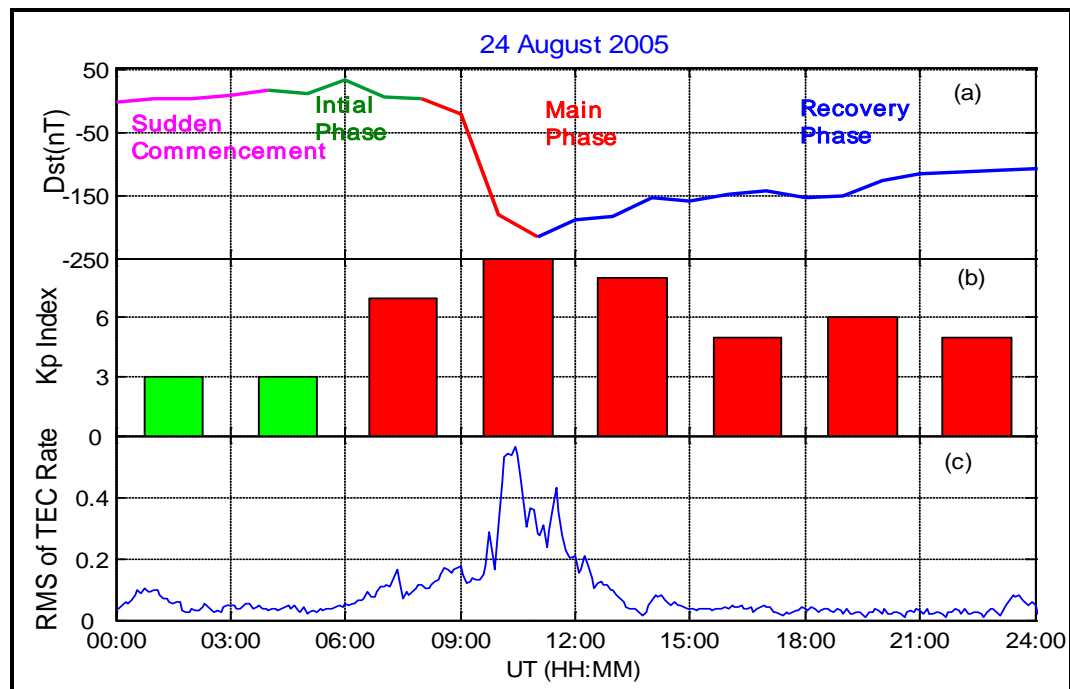


Fig. (3). (a) Dst variation, (b) Kp index variation and (c) RMS of TEC Rate variation on 24 August 2005.

We discussed the statistical reliability in terms of mean, standard deviation, range, and maximum value at two different interval of time, one between 00:00 UT to 12:00 and the second between 12:00 to 24:00 UT. Table 1 shows that the maximum RMS value is larger between 00:00 UT to 12:00 than it is between 12:00 UT to 24:00 UT. The standard deviation of RMS of TEC was observed to be 0.09. The effect of RMS on the absolute position error can be correlated with the position error, as it rose up to 3.218 meters and then decreased to 2.153 m after 12:00 UT. The average number of satellites visible in both cases is 9.229 and 9.1, respectively. The DOP depends on the total number of visible satellites and their angle elevation, and in both cases the statistics do not show a large difference. On average, the DOP was observed to be low, between 12:00 UT to 24:00 UT. The overall statistics show that the accuracy of precise positioning and satellite geometry are degraded as the RMS of TEC is increased. As we have observed in Fig. (3), the recovery phase commenced after 12:00 UT and statistics analysis clearly shows that between 00:00 UT and 12:00 UT, positional accuracy and satellite geometry degradation was high compared to 12:00 UT to 24:00 UT.

**DISTURBED IONOSPHERE**

15 September 2005 was an ionospheric disturbed day; the magnetic storm was observed at 08:35 UT (Fig. 5a) as SSC. With the initial phase of storm, the Kp index showed a value greater than 4, shown in Fig. (5b). During this event at 17:00 UT, the Dst reached its maximum negative value of -86 nT and the global ground-based magneto meter also indicated similar significance, as the value of the Kp index reached to 7. Fig. (5c) shows the corresponding RMS values of the rate of change of TEC for all visible satellites calculated for every 5 minutes on 15 September 2005. The RMS of VTEC gives an idea about the occurrence of ionospheric irregulari-

ties. The RMS value shows small enhancement between 08:00 to 16:00 UT, and reached to maximum peaks at 17:00 UT with continuous enhancement up to 24:00 UT.

To quantify the effect of ROT fluctuation on GPS positioning and satellite geometry, in Fig. (6) we observed a horizontal positioning error for a fixed GPS receiver and DOP parameters. The format of Fig. (6) is the same as that of Fig. (4). From 00:00 UT to 04:00 UT, when the RMS value was less than 0.1, the positional error was observed to be less than 2 m. At 04:00 UT and 08:00 UT, a small enhancement in the RMS was observed and the absolute horizontal positional error up to 2 m, which corresponds with this enhancement. As soon as the RMS seemed to be more than 0.2, between 18:00 UT and 22:00 UT, the result became worse in terms of absolute horizontal error, which reached up to 4 meters, as shown in the scatter plots of easting and northing error. Most of the scatter points representing easting and northing error come outside 99.9% of the confidence circle. The value 3DRMS is 2.7147 m (which is 99.97% of the confidence level) and CEP 1.0978 (49% of the confidence level) for the whole day, which is very large for precise positional analysis. Due to the presence of ionospheric disturbances, the number of satellites locked dropped down to a minimum value of 6 between 14:00 to 18:00 UT, as indicated in the upper right panel of the figure. A lower right panel shows that every time there is an enhancement in the absolute horizontal position error, the DOP parameters also increase; this signifies the degradation of satellite geometry. Fig. (6) shows a good correlation between RMS of ROT, positional error, and satellite geometry.

Table 2 records the statistical accuracy of the error in position and satellite geometry during disturbed ionospheric conditions, 15 September 2005. The maximum RMS value is higher between 12:00 UT and 24:00 UT as compared to 00:00 UT and 12:00 UT. As part of the effect of RMS on the

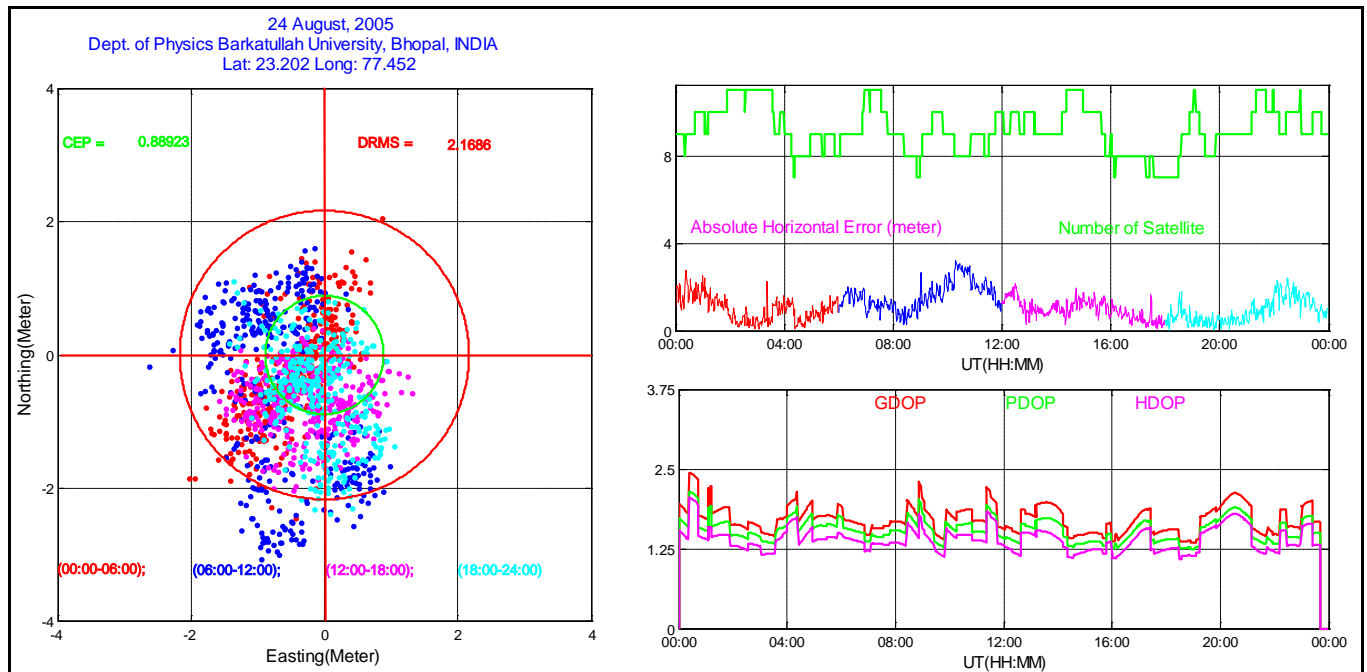
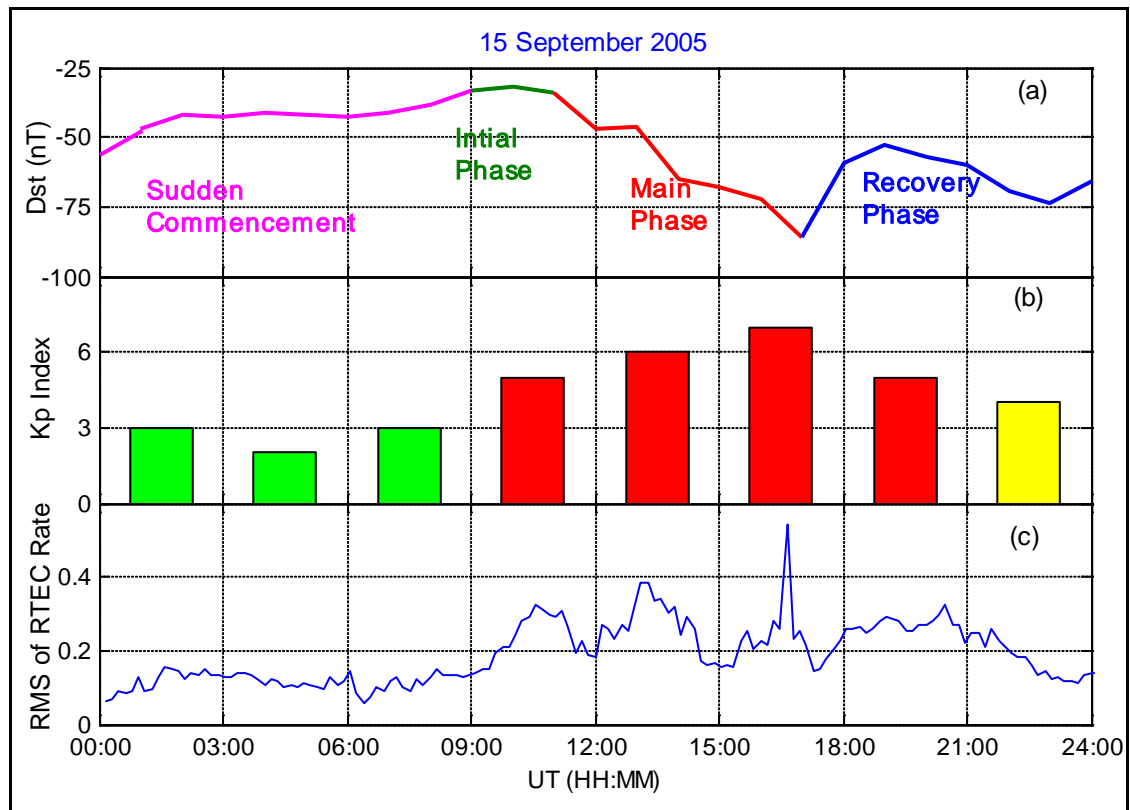


Fig. (4). (Left Panel) Error in Horizontal Plane (meter), (upper right panel) Number of Satellite Locked and Absolute Position Error (meter), (lower right panel) GDOP, PDOP and HDOP on 24 August 2005.

**Table 1. Position Error (Meter) and Satellite Geometry, on 24 August 2005, from 00:00 to 12:00 and 12:00 to 24:00 UT**

Date/Time → 24 August 2005	00:00 UT to 12:00 UT				12:00 UT to 24:00 UT			
Observations	Mean	Std	Range	Max	Mean	Std	Range	Max
RMS of dTEC	0.0808	0.099	0.53	0.563	0.0385	0.02	0.19	0.205
Absolute Error	1.579	0.6272	2.948	3.218	0.9696	0.4227	2.093	2.153
GDOP	1.688	0.2905	2.439	2.439	1.498	0.213	0.983	2.219
PDOP	1.827	0.1504	0.999	2.142	1.402	0.101	0.899	1.996
HDOP	1.377	0.1429	0.694	2.051	1.185	0.131	0.531	1.992
Number of Satellite	9.229	1.067	4	11	9.1	1.08	4	11



**Fig. (5).** (a) Dst variation, (b) Kp index variation and (c) RMS of TEC Rate variation on 15 September 2005.

absolute position error, it was observed up to 2.6 meters before 12:00 UT but, after that, the error reached up to 4.1 meters with a standard deviation of approx 1, which is higher as compared to the first part of the statistics. The mean number of satellites visible was 9.283 before 12:00 UT and decreased to 8.636 after 12:00 UT due to the presence of ionospheric disturbances. Satellite geometry was also affected, as shown in GDOP, Position Dilution of Precession (PDOP) and Horizontal Dilution of Precession (HDOP) statistics. These statistics show that the accuracy of precise positioning and satellite geometry are degraded as the RMS of TEC is increased.

**QUIET IONOSPHERE**

Fig. (7a) illustrates the Dst variation for an ionospherically quiet day, on January 25, 2005; it was, in fact, the quietest day of the year. On this day, the Dst was very quiet

with a maximum negative value of up to -33 nT, and the Kp index remained below 2 throughout the day (Fig. 7b). A time series of RMS of ROT values for all visible satellites calculated for every 5 minutes on 25 January 2005 is plotted in Fig. (7c). For the whole day the RMS remained less than 0.1, which represents the quiet state of ionospheric activity and has also been cross checked with Dst and Kp index. To see the effect of quiet ionospheric conditions on the horizontal position error and on satellite geometry, Fig. (8) is displayed.

On this particular day, the easting and northing error are within +2 meters and the DRMS value is also very low, at 1.8774. Most of the points of positional error are within the confidence level of 99.97%. This is well observed in the absolute horizontal error plot mentioned on right upper panel; during this event there were no virtual variations and the absolute horizontal error was recorded as being within 2 meters for the almost whole day. The number of satellites

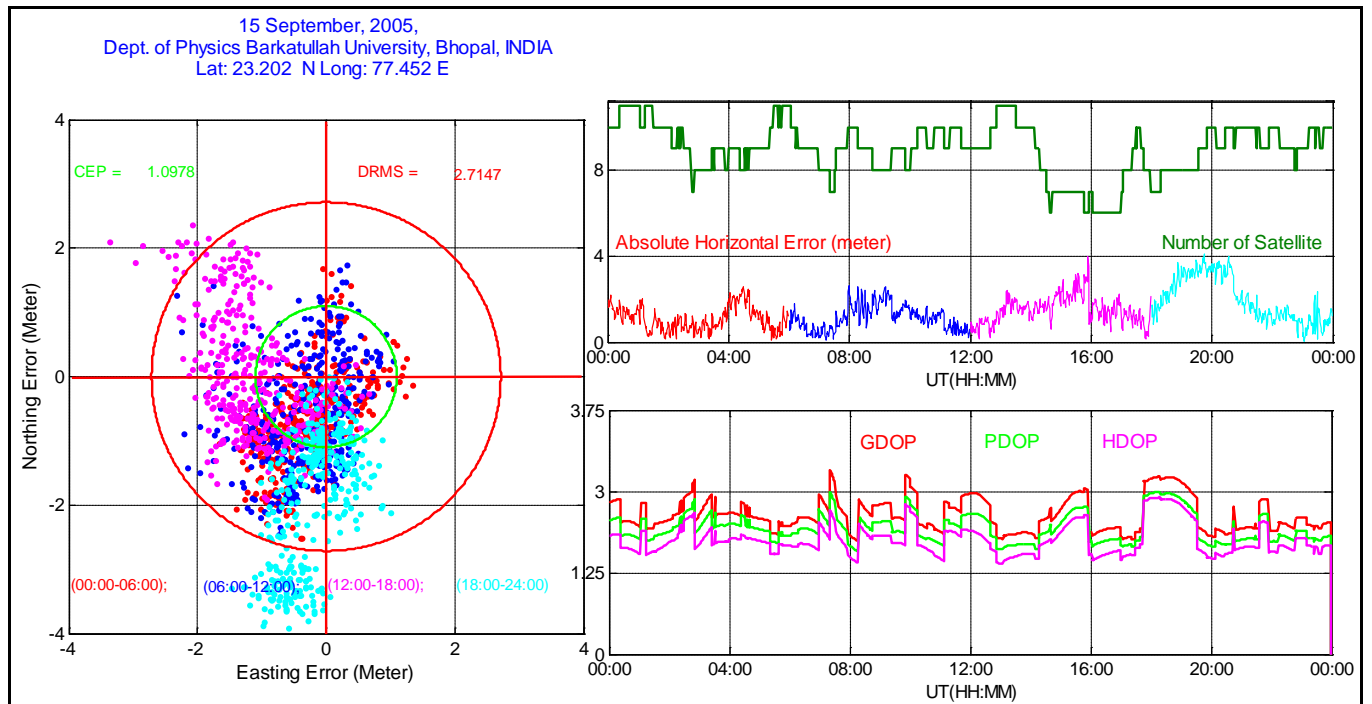


Fig. (6). (Left Panel) Error in Horizontal Plane (meter), (upper right panel) Number of Satellite Locked and Absolute Position Error (meter) (lower right panel) GDOP, PDOP and HDOP on 15 September 2005.

locked was  $\geq 8$ . Due to the sufficient number of locked satellites, and in the absence of any ionospheric disturbance, the DOP parameters remained smooth for the whole day and showed good geometry.

Table 3 shows the statistics of the above results. It must be noted that very small differences were observed between 00:00 to 12:00 UT and 12:00 to 24:00 UT, due to the absence of ionospheric activity during the whole day. The maximum range error was 0.056, which was too small to generate any error of position solution. In the absence of ionospheric disturbances, the absolute error is less than 2.

To investigate the yearly statistics of positional error, the histogram of absolute horizontal error and the northing and easting errors of the considered events had been studied separately, the disturbed and one for the quiet ionosphere conditions, as shown in Fig. (9). The upper panel of Fig. (9) shows horizontal, north, and east errors for the disturbed ionosphere, while the left panel is for the quiet ionosphere.

As the plots signify, in a disturbed ionosphere the total number of absolute horizontal error events is more as compared to a quiet ionosphere. During disturbed ionospheric conditions, the magnitude of horizontal error was + 4 m, while during quiet ionospheric conditions it was less than + 2.3 m. Similarly, for northing and easting errors the number of occurrences is greater in a disturbed ionosphere as compared to a quiet ionosphere. During disturbed ionospheric conditions, the magnitude of northing and easting errors was + 5 m. However, during quiet ionospheric conditions, the errors were within 1-2.5 m, while for a disturbed ionosphere it was 2.5 m.

Table 4 shows the yearly statistical analysis of accuracy of the positional error and satellite geometry during quiet and disturbed ionospheric conditions. The absolute position error was recorded up to 1.9 m as a maximum value during quiet ionospheric conditions. The case is much more adverse during the disturbed ionospheric condition, as the maximum value of error reached was up to 5.473 m.

Table 2. Position Error (Meter) and Satellite Geometry, on 15 September 2005, from 00:00 - 12:00 and 12:00 - 24:00 UT

Date/Time → 15 September 2005	00:00 UT to 12:00 UT				12:00 UT to 24:00 UT			
Observations	Mean	Std	Range	Max	Mean	Std	Range	Max
RMS of dTEC	0.0314	0.039	0.197	0.2104	0.0785	0.062	0.296	0.329
Absolute Error	1.107	0.565	2.559	2.653	1.753	0.9013	4.065	4.1
GDOP	2.257	0.1599	4.866	2.257	1.69	0.2414	0.78	2.188
PDOP	1.965	0.1301	0.725	1.991	1.996	0.2124	0.7092	1.996
HDOP	1.739	0.1344	0.717	1.839	1.405	0.2308	0.8174	1.926
Number of Satellite	9.283	0.9683	4	11	8.636	1.41	5	11

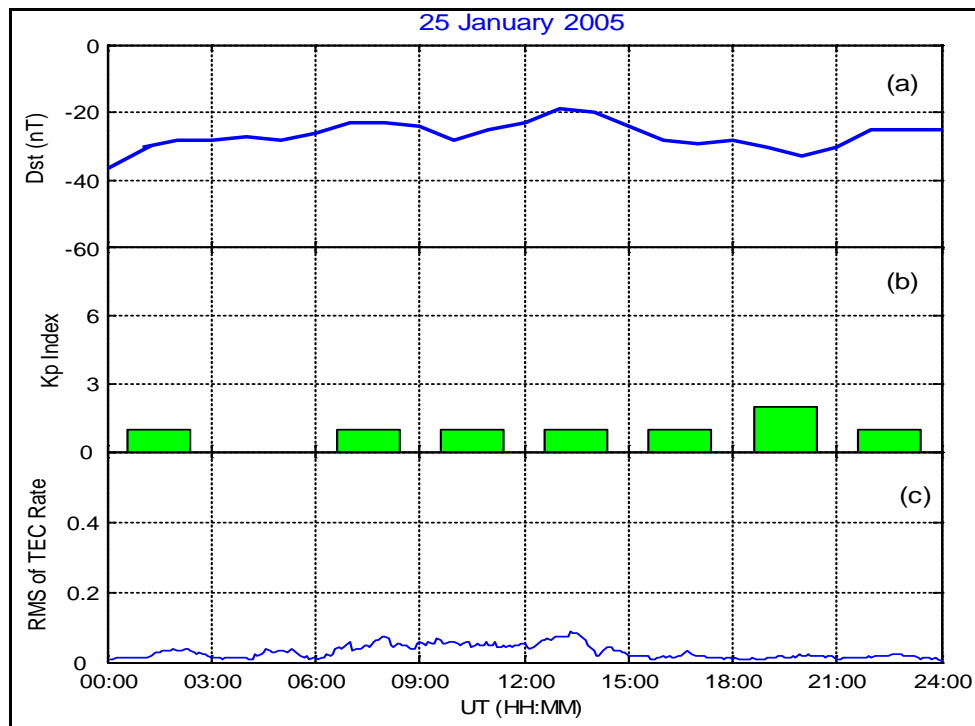


Fig. (7). (a) Dst variation, (b) Kp index variation and (c) RMS of TEC Rate variation on 25 January 2005.

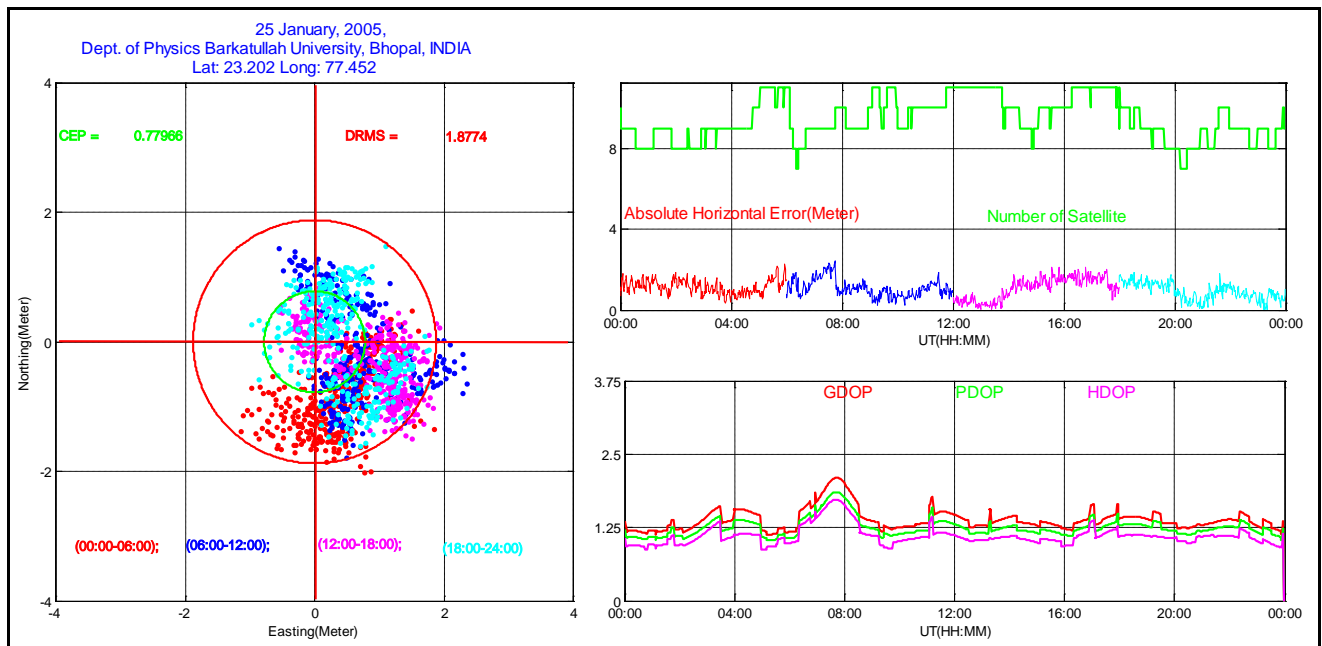


Fig. (8). (Left Panel) Error in Horizontal Plane (meter), (upper right panel) Number of Satellite Locked and Absolute Position Error (meter), (lower right panel) GDOP, PDOP and HDOP on 25 January 2005.

The Cumulative Probability distribution functions for RMS of TEC Rate and Horizontal error are plotted in Fig. (10). During disturbed ionospheric conditions, the 90 % of probability of RMS of TEC Rate is 0.3, which correspond to horizontal error as 3.9 m. In the 50 % cases the probability of occurrence of horizontal error is 1.5 m, whereas the RMS of TEC is 0.13, as shown in the upper and lower left panel respectively. Similarly, during the quiet ionosphere, the 90% of RMS of TEC Rate is below 0.15, as shown in the upper right panel of Fig. (10); its effect is observed on horizontal

error with 90% of error with almost less than 2 m (lower right panel). These plots clearly signify the effect of ROT on the precise position of GPS receiver.

Fig. (11) shows the cumulative probability distribution function for GDOP, PDOP, and HDOP for disturbed and quiet ionosphere. We found that when the ionosphere was disturbed, the GDOP, PDOP, and HDOP values were 1.7, 1.5, and 1.0, respectively. This cumulative distribution curve shows that 50.0% of the DOP values lie between 1.8 to 2.4



Table 3. Position Error (Meter) and Satellite Geometry on 25 January, 2005 from 00:00 - 12:00 & 12:00 - 24:00

Date/Time → 25 January 2005	00:00 UT to 12:00 UT				12:00 UT to 24:00 UT			
Observations	Mean	Std	Range	Max	Mean	Std	Range	Max
RMS of dTEC	0.0314	0.017	0.165	0.051	0.0785	0.016	0.164	0.056
Absolute Error	0.912	0.282	1.996	2.109	1.00	0.1072	1.813	1.935
GDOP	1.39	0.033	1.257	1.98	1.379	0.0414	0.78	1.14
PDOP	1.285	0.0728	1.029	1.828	1.276	0.098	0.6657	1.728
HDOP	1.259	0.058	0.381	1.27	1.25	0.066	0.6459	1.027
Number of Satellite	9.335	0.9598	4	11	9.569	1.13	4	11

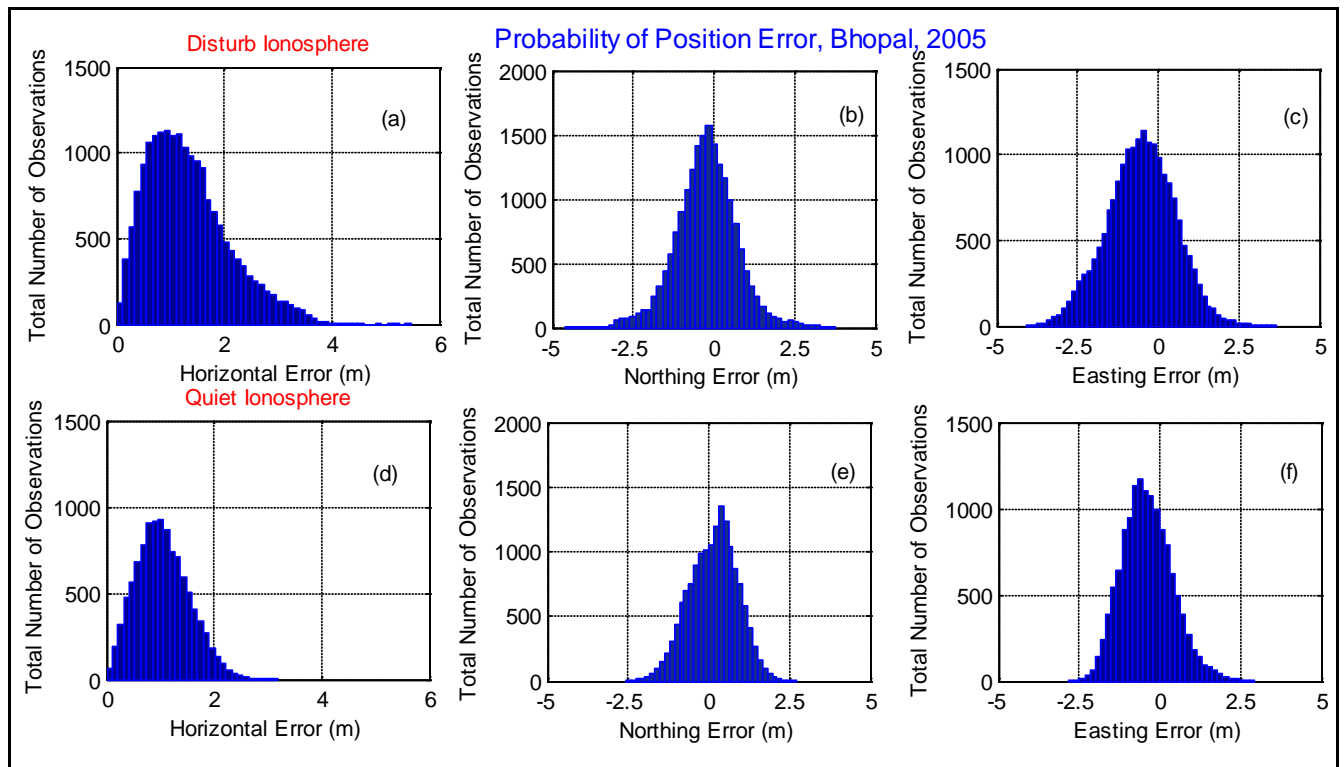


Fig. (9). Probability of Disturbed & Quite ionosphere.

and 90.0% of the DOP values are within the range of 2.3 to 3. The largest value occurred as 4.0, 3.1, and 2.943 for GDOP, PDOP, and HDOP, respectively. On the other hand, during the quiet ionosphere the smallest GDOP, PDOP, and HDOP were 1, 0.8, and 0.57, respectively. For better accuracy these values are quite good.

**SUMMARY AND DISCUSSION**

At present, when the selective availability is turned off, the ionospheric effects are considered to be the largest source of error for high level accuracy of GPS positioning and navigation. It is now confirmed by research that for single frequency users, the ionosphere is the main drawback in achieving a high level of accuracy in positioning. The various studies show that users of dual-frequency GPS receivers will be affected less as compared to single frequency users.

In this paper, dual frequency GPS data from a low-latitude station, Bhopal, during the low solar activity of 2005 has been analyzed. The effect on GPS signals as they pass through the ionosphere is the largest single source of error. The Earth’s ionosphere is capable of corrupting the navigation application. GPS satellites orbiting at altitudes of 20,000 km can be disrupted by disturbances in the ionospheric F-region below 1,000 km [15]. Such disturbances in propagation result mainly from night-time plasma irregularities, which can be particularly troublesome in the equatorial region and during times of high solar activity; the navigation becomes degraded and even complete signal loss may be observed. The ionospheric range error can dominate the DGPS error budget under high levels of ionospheric activity.

This paper presents the probability of the occurrence of positional error and satellite geometry in both quiet and disturbed ionospheric conditions. To achieve a better under-

**Table 4. Statistic Test for Effect of ROT on GPS Precise Positioning**

Statistics	Disturb Ionosphere				Quiet Ionosphere			
	Mean	Std	Range	Max	Mean	Std	Range	Max
Horizontal Error	1.1872	0.766	5.462	5.473	0.708	0.156	1.996	1.9
RMS of dTEC	0.3255	0.054	0.295	0.668	0.010	0.004	0.1191	0.1317
GDOP	2.71	0.3832	2.053	4.984	1.331	0.037	0.1681	1.499
PDOP	1.585	0.2642	1.939	3.893	1.312	0.031	0.146	1.374
HDOP	1.414	0.2486	1.853	3.596	1.147	0.038	0.186	1.222
Number of Satellite	7.194	1.105	5	11	9.303	0.073	3	11
DRMS	2.748	0.3887	1.068	3.571	1.342	0.056	0.585	1.847
CEP	1.13	0.1327	0.426	1.435	0.589	0.038	0.249	0.8232

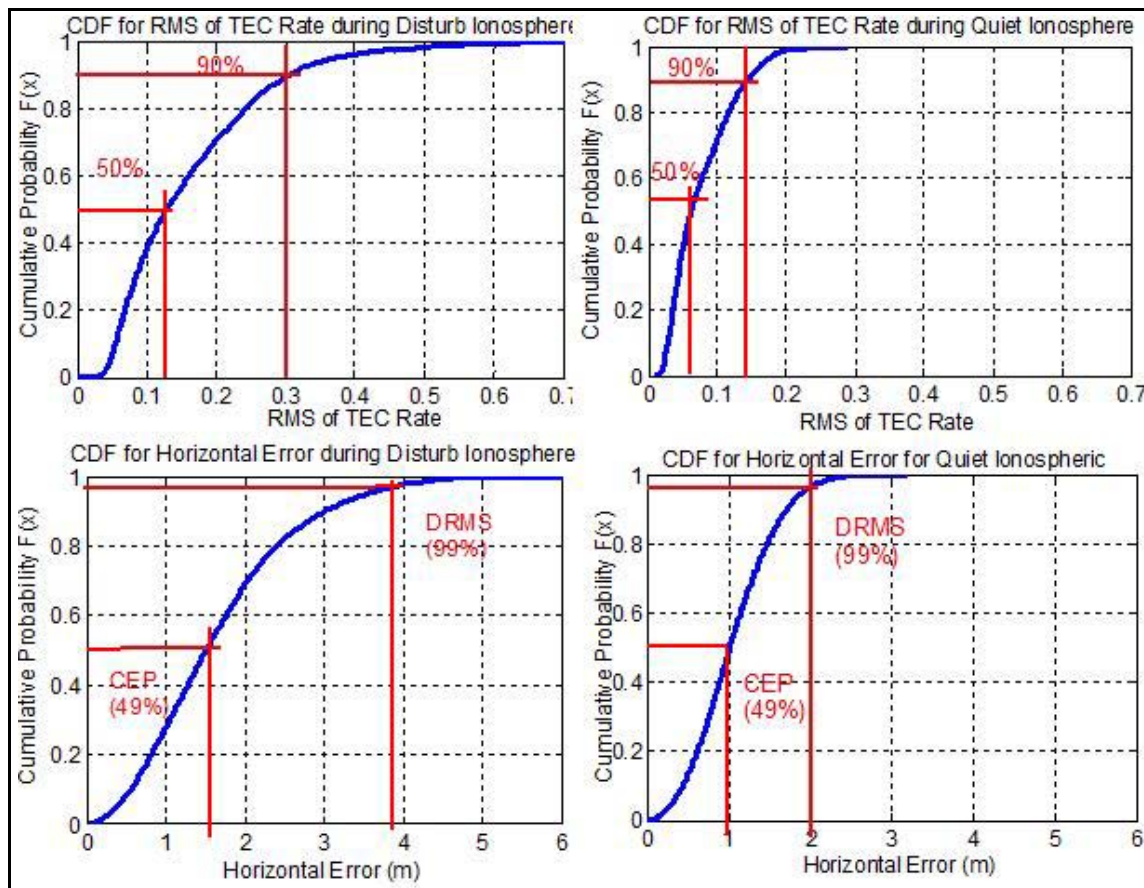


**Fig. (10).** Cumulative distribution function RMS & Horizontal error.

standing, we calculate RMS of TEC Rate, horizontal error, CEP, DRMS, DOP parameters, and total number of satellites locked. Our study shows that during the solar minimum year of 2005, the maximum value of RMS of TEC Rate was 0.13 in a quiet ionosphere, while it was 0.6678 in a disturbed ionosphere. The study shows that the strong fluctuations in TEC were caused by the presence of large-scale ionospheric structures of enhanced electron density. Based on GPS satellite data, researchers have observed that satellite signals are strongly scattered in the presence of intense small-scale irregularities of the ionospheric F2-layer at equatorial latitudes, resulting in fast variations in TEC [16-19].

We found that during quiet ionospheric conditions, the horizontal error was less than 2 meters, but the situation became adverse during disturbed ionospheric conditions, with the maximum error reaching up to 5-6 meters. The irregular TEC component makes a substantial contribution in this case. The amplitude of random TEC variations, with a period from a few minutes to several hours in conditions of geomagnetic disturbances, can make up as much as 50% of the background TEC value [20-22].

A magnetic storm on 24 August 2005 showed that during the main phase of a storm, a sudden enhancement in positional error is observed. At the equatorial region, due to

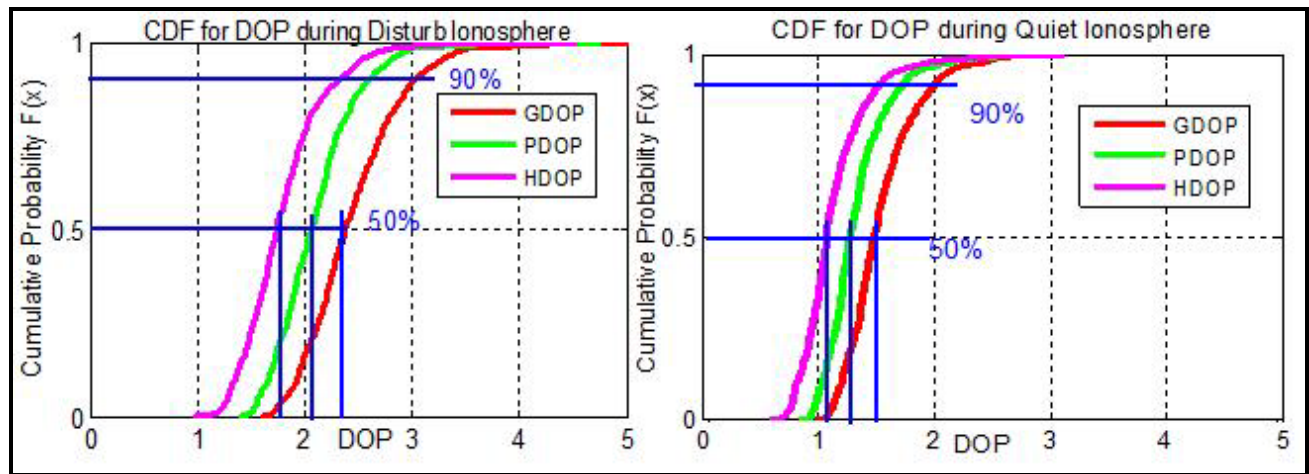


Fig. (11). Cumulative distribution function GDOP, PDOP, HDOP.

the occurrence of intense small-scale irregularities of the ionospheric F2-layer, fast variations in TEC developed and caused the degradation of positioning accuracy and quality of GPS performance. Afraimovich *et al.* found that growth of the level of geomagnetic activity is accompanied by growth of the total intensity of TEC variations. These variations are observed due to fluctuations in TEC in the ionosphere. We found that a positional error of up to 1 m is common during quiet and disturbed ionospheric conditions; the probability of maximum occurrence of positional error is two times greater in disturbed ionospheric conditions as compared to a quiet ionosphere [23].

During geomagnetic disturbances in near space, deterioration of GNSS operation quality appeared and, as a consequence, a reduction of positioning accuracy and the occurrence of subsequent failures, in ground-based users' coordinates have been observed [24]. Aarons shows that the main degradation comes from the systematic ionospheric effects of radio wave propagation: the group and phase delay and the frequency Doppler shift. In many instances the degree of manifestation of the above effects has only a weak dependence on the local distribution of electronic density in the ionosphere, but is directly correlated with the value of total electron content (TEC) along the radio signal propagation path [25].

A Strong TEC fluctuation decreased the total number of satellites locked in disturbed ionospheric conditions, the effects of which were observed, for a few seconds, in satellite geometry. The main factors affecting DOP are the number of satellites being tracked and where these satellites are positioned in the sky. Our statistical study shows that in a disturbed ionosphere, when the average number of satellites locked is 7.194, the maximum value of GDOP, PDOP, and

HDOP are varied between 3 and 4—which is high as compare to quiet ionospheric conditions. The quality of a GPS-derived position estimate depends upon both the measurement geometry as represented by DOP values, and range errors caused by signal strength, ionospheric effects, multipath, etc. The presence of ionospheric irregularities can cause degradation in the GPS navigational accuracy and limitations in the GPS system tracking performance [26-27].

At the low latitude region, strong ionospheric disturbances occurred frequently in a solar maximum that dramatically increased the measurement noise level and number of lost locked GPS signals [28]. Previous research shows the impact of the ionosphere, which is the most important cause of satellite positioning errors [29-30]. General sources of satellite positioning errors are well identified [31-32]. Under high levels of ionospheric activity, the ionospheric range error can dominate the GPS error budget and can cause degradation of GPS receiver tracking performance and, in extreme cases, loss of navigation capabilities. Essentially, free electrons contained in the ionosphere affect the propagation of the signal as it passes through. Since the signals are traveling at the speed of light and GNSS is based on nanosecond timing, it does not take much interference to introduce error. In order to provide robust and reliable positioning, a strict control of the causes of satellite positioning errors is demanded [33]. The paper concludes that during a low solar activity period, the positional error can be observed using a dual frequency receiver. The next solar cycle will occur in the years 2011-2012, and it will be more difficult for GPS users to find precise positioning. Further study and better correction are required for precise positioning.

#### ACKNOWLEDGEMENT

One of the authors, Soumi Bhattacharya, wishes to acknowledge the financial support from NCAOR, Goa, Ministry of Earth Science, Govt. of India, under their project: Space Weather Programme at Antarctica. The authors also acknowledge the UK Solar System Data Center for providing Kp data (web page: [http://www.ukssdc.ac.uk/wdcc1/geophy\\_menu.html](http://www.ukssdc.ac.uk/wdcc1/geophy_menu.html)), [ukssdc.ac.uk/wdcc1/geophy\\_menu.html](http://ukssdc.ac.uk/wdcc1/geophy_menu.html)), and also acknowledge the WDC for Geomagnetism, Kyoto for providing Dst data, and Google earth for providing the satellite view of GPS point.

#### REFERENCES

- [1] Davies K. Ionospheric Radio; IEE Electromagnetic Waves Series Peter Peregrinus Ltd., 1990.
- [2] Aarons J, Mendillo M, Yantosca R. GPS phase fluctuations in the equatorial region during the MISETA 1994 campaign. *J Geophys Res* 1996; 101(26): 851-62.
- [3] Kelley MC, Hysell D, Musman S. Simultaneous Global Positioning System and radar observations of equatorial spread F at Kwajalein. *J Geophys Res* 1996; 101: 2333-42.

- [4] Weber EJ, Basu S, Bullett TW, *et al.* Equatorial plasma depletion precursor signatures and onset observed at 11° south of the magnetic equator: *J Geophys Res* 1996; 101: 26829-38.
- [5] Aarons J, Mendillo M, Yantosca R. GPS phase fluctuations in the equatorial region during sunspot minimum. *Radio Sci* 1997; 32: 1535-50.
- [6] Hunsucker RD, Coker Clayton, Cook Jeffrey, Gus Lott. An investigation of the feasibility of utilizing GPS/TEC signatures for near real time forecasting of auroral-E propagation at high -HF and low-VHF frequencies. *IEEE Trans Ant Prop* 1995; 43: 1313-18.
- [7] Coco DS, Gaussiran TL, Coker C. Passive detection of sporadic E using GPS phase measurements. *Radio Sci* 1995; 30: 1869-74.
- [8] Groves KM, Basu S, Weber EJ, *et al.* Equatorial scintillation and systems support. *Radio Sci* 1997; 32 (5): 2047-64.
- [9] Wanninger L. Effects of the equatorial ionosphere on GPS. *GPS World*. 1993; 44(7): 2047-64.
- [10] Miyazaki S. Expansion of GSI's nationwide GPS array. *Bull Geogr Surv Inst* 1997; 43: 23-34.
- [11] Afraimovich EL, Kosogorov EA, Leonovich LA, Palamartchouk KS, Perevalova NP, Pirog OM. Determining parameters of large-scale traveling ionospheric disturbances of auroral origin using GPS-arrays. *J Atm Sol Terr Phys* 2000; 62(7): 553-65.
- [12] Otsuka Y, Ogawa T, Saito A, Tsugawa T, Fukao S, Miyazaki S. A new technique for mapping of total electron content using GPS network in Japan. *Earth Planets Space* 2002; 54: 63-70.
- [13] Pi X, Mannucci AJ, Lindqwister UJ, Ho CM. Monitoring of global ionospheric irregularities using the worldwide GPS network. *Geophys Res Lett* 1997; 24: 2283-86.
- [14] Hargreaves JK. *The solar-terrestrial environment*; Cambridge University Press, Cambridge, 1992.
- [15] Klobuchar J. Ionospheric effects on GPS. In: Parkinson BW and Spilker JJ. (Eds). *Global Positioning System: theory and applications*. American Institute of Aeronautics and Astronautics Inc.: Washington, 1996.
- [16] Aarons J. Global morphology of ionospheric scintillations. *Proc IEEE* 1982; 70(4): 360-78.
- [17] Aarons J, Mendillo M, Kudeki E, Yantosca R. GPS phase fluctuations in the equatorial region during the MISETA 1994 campaign. *J Geophys Res* 1996; 101(12): 26851-62.
- [18] Aarons J, Mendillo M, Yantosca R. GPS phase fluctuations in the equatorial region during sunspot minimum. *Radio Sci* 1997; 32: 1535-50.
- [19] Aarons J, Lin B. Development of high latitude phase fluctuations during the January 10, April 10-11, and May 15, 1997 magnetic storms: *J Atmos Terr Phys* 1999; 61: 309-27.
- [20] Basu S, Basu S, MacKenzie E, Whitney HE. Morphology of phase and intensity scintillations in the auroral oval and polar cap. *Radio Sci* 1985; 20(3):347-56.
- [21] Bhattacharya A, Beach TL, Basu S, Kintner PM. Nighttime equatorial ionosphere: GPS scintillations and differential carrier phase fluctuations. *Radio Sci* 2000; 35: 209-24.
- [22] Warnart R. The study of the TEC and its irregularities using a regional network of GPS stations, *IGS Worksh Proc* 1995; 249-63.
- [23] Afraimovich EL, Altyntsev AT, Grechnev VV, Leonovich LA. Ionospheric effects of the solar flares as deduced from global GPS network data. *Adv Space Res* 2001c; 27: 1333-38.
- [24] Afraimovich EL, Demyanov VV, Kondakova TN. Degradation of performance of the navigation GPS system in geomagnetically disturbed conditions. *GPS Solutions* 2003; 7(2): 109-19.
- [25] Aarons J. Global morphology of Ionospheric Scintillations. *Proc IEEE* 1982; 70(4): 360-78.
- [26] Bandyopadhyay T, Guha A, Das A, Gupta P, Banerjee A, Bose A. Degradation of navigation accuracy with global positioning system during period of scintillation at equatorial latitudes. *Electron Lett* 1997; 33(12): 1010-11.
- [27] Skone SH. The impact of magnetic storm on GPS receiver performance. *J Geodesy* 2001; 75(6): 457-68.
- [28] Chen W, Shan G, Congwei Hu, Yongqi Chen, Xiaoli Ding. Effect of ionospheric disturbances on GPS observation in low latitude area. *GPS Solution* 2008; 33-41.
- [29] Parkinson BW, Enge PK. *Differential GPS*. In: Parkinson BW, Spilker JJ, Eds. *Global positioning system: theory and applications, vol II*. American Institute of Aeronautics and Astronautics, Washington, DC. 1996; 3-50.
- [30] Klobuchar JA. Ionospheric time-delay algorithm for single-frequency GPS users: *IEEE Trans Aerosp Electron Syst* 1987; 23(3): 325-31.
- [31] Parkinson BW, Spilker JJ Jr, Eds. *Global Positioning System: Theory and Applications: AIAA; Washington, DC. 1996; Vol 1*.
- [32] Misra P, Enge P. *Global Positioning System: Signals, Measurements, and Performance (2nd printing)*: Ganga-Jamuna Press; Lincoln, MA. 2004.
- [33] Sandford WH. The Impact on Solar Winds on Navigation Aids. *J Navig* 1999; 52: 42-46.

Received: November 3, 2008

Revised: November 24, 2008

Accepted: November 27, 2008

© Tiwari *et al.*; Licensee *Bentham Open*This is an open access article licensed under the terms of the Creative Commons Attribution Non-Commercial License (<http://creativecommons.org/licenses/by-nc/3.0/>) which permits unrestricted, non-commercial use, distribution and reproduction in any medium, provided the work is properly cited.